Article

Relationship between the Composition and Elastic Modulus of TiZrTa Alloys for Implant Materials

Jinzhu Zhao [1], Kaiyang Liu [2], Meining Ding [2], Lixia Yin [2] and Shunxing Liang [2,3,4,*]

[1] Department of Material Engineering, Hebei Construction Materials Vocational and Technical College, Qinhuangdao 066002, China
[2] School of Materials Science and Engineering, Hebei University of Engineering, Handan 056038, China
[3] Hebei Key Laboratory of Wear-Resistant Metallic Materials with High Strength and Toughness, Hebei University of Engineering, Handan 056038, China
[4] Hebei Engineering Research Centre for Rare Earth Permanent Magnetic Materials & Applications, Hebei University of Engineering, Handan 056038, China
* Correspondence: liangshx@hebeu.edu.cn

Abstract: The elastic modulus is a key factor influencing the applications of implant materials because of the weakening effect of stress shielding. Ti and its alloys are good potential implant materials thanks to their low elastic modulus and fine biocompatibility. The addition of alloying elements into pure Ti and Ti alloys is the basic way to further decrease the elastic modulus whilst simultaneously enhancing strength, wearability, and corrosion resistance, for example. Finding the relationship between the composition and elastic modulus can greatly promote the development of Ti alloys with a low modulus for implant applications. In the current work, we investigated the elastic modulus of TiZrTa alloys with scores of compositions by using the high-throughput diffusion couple method, nanoindentation, and an electron probe micro-analysis. The relationship between the elastic modulus and the composition of the TiZrTa alloys was obtained. The average valence electron theory was employed to make clear the variation between the elastic modulus and the composition. Finally, the composition range formulae of TiZrTa alloys likely to have a low modulus were established by combining our data and previous results. These findings are helpful in developing new Ti alloys with a low modulus and also help to further understand the alloying theory.

Keywords: Ti alloys; elastic modulus; composition; implant materials

1. Introduction

Titanium alloys are widely used in fields such as aerospace, medical, shipping, and chemical because of their low density, high strength, fatigue resistance, and good biocompatibility. Recently, Ti alloys as medical materials have attracted more and more attention thanks to their low elastic modulus, non-cytotoxicity, high strength, and corrosion resistance, for example [1–3]. The group of Niinomi committed to the mechanical properties of medical titanium alloys and supplied a few new beta Ti alloys with a low elastic modulus for preventing stress shielding between implant devices and bones [4–7]. Steinemann [8] and Kawahara [9] showed that the elements of Ti, Zr, Nb, Ta, and Pt exhibit excellent biocompatibility and biological activities with no cytotoxicity. Thus, many publications around low elastic Ti alloys with those elements have been reported such as the Ti-Nb series [10–13], the Ti-Zr series [14–16], and the Ti-Ta series [17–19] of alloys. Popov et al. [20] investigated the effect of heat treatments and plastic deformation on the structure and elastic modulus of an IMP-BAZALM (Zr-31Ti-18Nb (at.%)) biocompatible alloy. The micro-indentation showed that an elastic modulus lower than 60 GPa was obtained after a suitable treatment. The discussion proved that the appearance of the α'' and ω phases in the structure of the alloy led to an increase in the modulus of elasticity. The greatest increase in the modulus was observed under the conditions corresponding with the formation of the

ω phase. Liang et al. [21] summarized low modulus Ti alloys without cytotoxic alloying elements. The lowest elastic modulus of the developed Ti alloys, especially foam Ti alloys, was very close and even lower than biological bone (10~30 GPa). However, most of those results were obtained using trial-and-error methods or semi-empirical methods. Those methods can only select a few special composition points to have an attempt and are likely to omit potential compositions with better or ideal performances. Diffusion multiples is an efficient high-throughput method for alloy composition screening. Chen [22] investigated the diffusion coefficient and elastic modulus of Ti-X (Nb, Mo, Ta, and Zr) binary alloys through the diffusion multiples method and reported on the diffusion data and composition dependence of the elastic modulus of those binary Ti alloys. However, most previous reports have been used for binary Ti alloys. Recently, the diffusion multiples method was attempted to be used for the composition screening of ternary alloys and other component alloys. Ling et al. [23] investigated the variation in the modulus with the composition by using a Ti-Nb-Mo/Ti-Nb-Zr/Ta diffusion couple and obtained a possible composition range with a low modulus.

As mentioned above, cytotoxicity is a key factor before an application for biomaterials. For the development of low modulus Ti alloys, Zr, Nb, and Ta are the most used and widely confirmed alloying elements without cytotoxicity. Relatively speaking, the addition of Zr and Ta still has a great potential to develop Ti alloys with a low elastic modulus. It is well-known that Zr is a neutral element for the phase transition of Ti and its alloys. Thus, the addition of Zr alone into metal Ti should have no or very weak effects on its phase constitution, as Wang showed [24]. However, the addition of Zr together with other beta phase stabilizers of Ti alloys can enhance the stabilizing effect [25]. Furthermore, the addition of Zr can strengthen the mechanical properties. Thus, many investigators controlled the phase constitution and microstructure of Ti alloys through the addition of Zr together with other beta phase stabilizers such as Ti-Nb-Zr, Ti-Zr-Mo, and Ti-Zr-Al-V series alloys. However, an excessive Zr addition would entirely retain the beta phase whilst a few beta phase stabilizers are added together, making it difficult to control the phase constitution and microstructure. Previous works have proven that metastable beta Ti alloys should have a low elastic modulus [21]. Thus, it is valuable to investigate the relationship between the chemical composition and modulus of the TiZrTa series alloy and screen the chemical composition of TiZrTa alloys as potential implant materials.

In this work, the diffusion multiples method was applied to the TiZrTa ternary alloys. The relationship between the composition and elastic modulus of that series of alloys was investigated. Our other aim was to find low elastic modulus TiZrTa ternary alloys as potential biomaterials for hard tissue implants. The findings may help to promote the application of Ti alloys with a low elastic modulus. The results can also supply references for the development of Ti alloys with a low elastic modulus.

2. Materials and Methods

Pure metal nuggets of Ti, Zr, and Ta with a purity of 99.99 at.% were used as the raw materials. Those high-pure metal nuggets were bought from the China New Metal Materials Technology Co., Ltd. The chemical compositions of the pure metal nuggets are listed in Table 1. The metals of Ti and Zr were weighed with a ratio of 61.16:38.84; namely, the atomic ratio of 75:25. The weighed Ti and Zr were melted by using a non-consumable arc melting furnace under an argon atmosphere. Before melting, the furnace was vacuumed to 5×10^{-5} Pa and then filled with argon; this was repeated three times. Considering the uniformity of the composition, the ingots were turned over and remelted four times. Disc specimens with a diameter of 5 mm and a thickness of 3 mm were cut from those uniform ingots, as shown in Figure 1a. The specimens of Ta with the same size as the $Ti_{75}Zr_{25}$ alloy were directly cut from the commercial pure Ta. Those disc specimens, including $Ti_{75}Zr_{25}$ and Ta, underwent grinding, polishing, cleaning, and drying surface cleaning processes to prepare the diffusion specimens, as shown in Figure 1b. After surface cleaning, those specimens were immediately transferred into the argon atmosphere. The diffusion

specimens were assembled into a pure Mo fixture, as shown in Figure 1c. Before assembling, a force of 7 kN was loaded onto the specimens to maintain a slight plastic deformation of Ta, of which the yield strength was 320 MPa [26], to ensure a tight contact between those two diffusion specimens. Cubic boron nitride powders were dispersed onto the surface of each connecting part to facilitate the demolding. The whole assembly was processed in a vacuum glove box with a press, which was also under the argon atmosphere, as shown in Figure 1d. After assembling, the specimens were annealed at 1000 °C for 100 h in a vacuum furnace under the argon atmosphere. Before annealing, the furnace was vacuumed to 5×10^{-5} Pa and then filled with argon; this was repeated three times. The annealed specimens were cut in half and underwent a preparation process of the metallographic specimen for the next modulus and composition measurements.

Table 1. The chemical composition of the pure raw metals used.

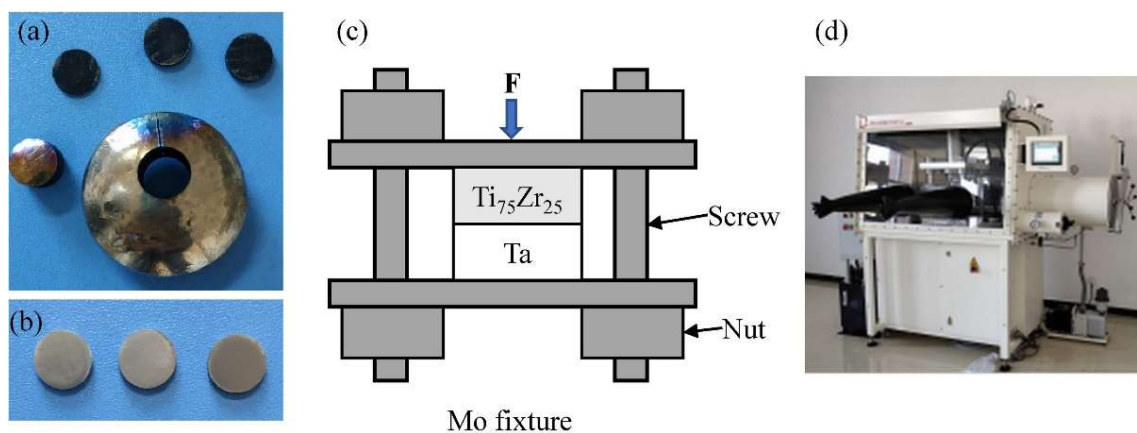| Impurity Elements (ppm)	Pure Metals		
	Ti	Zr	Ta
Al	-	<5	-
C	<5	<5	<1
Cd	-	<1	-
Co	<1	<5	-
Cr	<1	<5	<1
Cu	<1	<5	<1
Fe	<1	<10	<1
H	-	<5	<5
Mg	<1	<5	-
Mn	<1	<5	<1
Mo	<1	-	<1
N	<5	<5	<5
Nb	<1	-	<10
Ni	<1	-	<1
O	<5	<5	<5
Pb	<1	<1	-
S	<5	<5	<5
Si	<1	<1	<1
Sn	<1	-	-
Ta	<1	<1	Matrix
Ti	Matrix	<1	<1
V	<1	<5	-
W	<1	<5	<5
Zr	<5	Matrix	<1

Figure 1. Specimens and assembly pictures: (**a**) ingots; (**b**) diffusion specimens; (**c**) assembly diagram; and (**d**) a vacuum glove box with a press.

The elastic modulus of the specimens was obtained via a nanoindentation test [27,28], which is usually used to determine the elastic modulus of metals and alloys [29–31] An MTS Nanoindenter XP with a Berkovich indenter was used in this work. A constant loading rate/load of 0.05 s^{-1} was assigned to a depth of 1500 nm; the load was maintained for 30 s. After that, the indenter was unloaded at the same rate as the loading. The average modulus value within the indentation depths of 1000–1500 nm in the load-displacement curve was seen as Young's modulus. A nanoindentation test was performed from one side to the other side through the diffusion boundary with a distance step of 25 μm to avoid the overlapping effects between the indents and to improve the accuracy. A DSX 500-type Olympus 3D opto-digital microscope was employed to observe the morphology near the boundary of the diffusion couple. A JXA-8230-type electron probe micro-analysis (EPMA) was used to measure the composition profile. The conditions during the EPMA measurement were a 20 keV accelerating voltage, a 10 nA beam current, and a 5 μm beam spot. In order to agree with the hardness measurement points, the chemical composition was tested after the nanoindentation. The indents were found before the composition test and the chemical compositions on the parallel line of the indent test line were measured, as shown in Figure 2. The position corresponding with the first indent was tested as the first composition point. The same test step—namely, 25 μm for the nanoindentation test—was used to ensure that the composition measurements agreed with the hardness measurement points. In order to improve the accuracy, three chemical composition parallel lines were tested. The displayed chemical composition data were the average values of those three measurements.
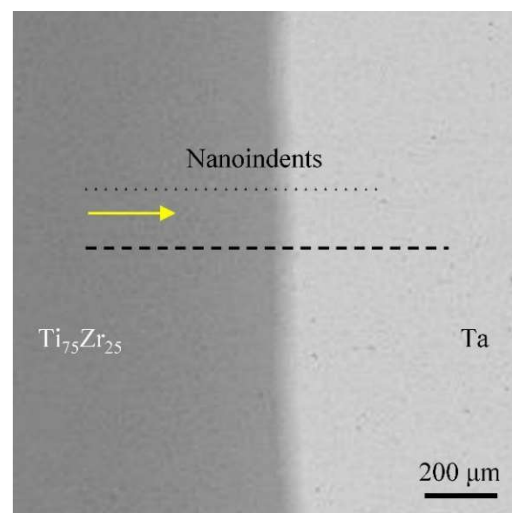

Figure 2. Optical microscopy image of annealed diffusion couple. Triangles are the nanoindents, the arrow is the test direction, the dashed line indicates the EPMA test location.

3. Results and Discussion

Figure 2 shows the optical microscopy image near the boundary of the diffusion couple after annealing at 1000 °C for 100 h. In that image, the boundary of the diffusion couple was blurry. That was because of the interdiffusion of the elements. The small triangles in Figure 2 were the indents of the nanoindentation tests. The arrow in Figure 2 shows the direction of the nanoindentation test. The first indent position was defined as the onset; namely, the distance was 0. A variation in the elastic modulus with the distance is shown in Figure 3a. The points with an elastic modulus over 100 GPa on the Ta-rich side are not shown. From Figure 3a, the elastic modulus was maintained around 103 GPa when the distance was below 200 μm. After that point, the modulus slowly decreased with an increase in the distance. When the distance was higher than 400 μm, the modulus sharply decreased. The lowest modulus value of 61.3 GPa appeared at a distance of 525 μm. As the test continued, the modulus tardily increased at first and then closed to 100 GPa. The EMPA scan location is also shown as a dashed line in Figure 2. As the elastic modulus of

the Ta-rich side was relatively high, the nanoindentation test stopped at a distance near 800 μm, which was still in the diffusion area. Thus, the EPMA test distance was longer than the nanoindentation. Compositions from 0 to 1000 μm were tested; the compositions at various distances are shown in Figure 3b. The alloying composition remained stable at distances below 200 μm and over 800 μm. A rapid variation in the composition was observed at distances between 625 μm and 650 μm. According to the diffusion theory, the composition should have sharply changed near the diffusion boundary. Thus, it could be inferred that the diffusion boundary of this couple should have been at a distance of 650 μm. Based on this deduction, and combined with the composition files in Figure 3b, the diffusion distances of Ti and Zr to Ta were approximately 450 μm, from 200 to 650 μm. That of Ta to $Ti_{75}Zr_{25}$ was approximately 150 μm, from 650 to 800 μm. This obvious difference in the diffusion distance mainly resulted from various diffusion coefficients. Liu et al. [32] reported the mobility of Ti in Ta and Ta in Ti through theoretical calculations and experimental verifications. The results showed that the mobility of Ta in Ti was fast. Thus, there would be a long tail on the Ti-rich side. Ansel et al. [33] also measured the diffusion composition files of a Ti/Ta couple annealing at 1500 °C for 3 h and showed similar results to this work.
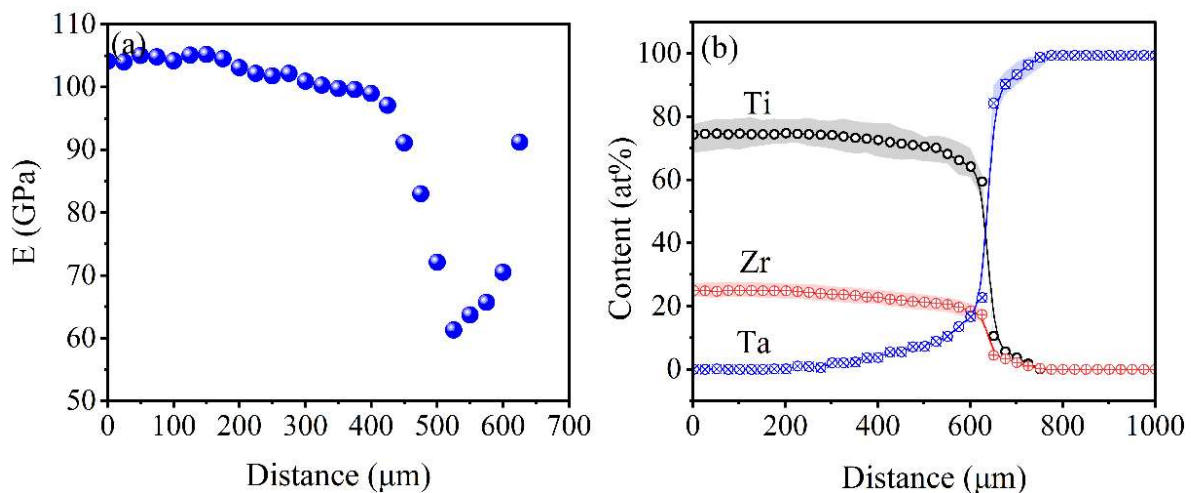

Figure 3. Variations in (**a**) modulus and (**b**) composition with distance. The shaded areas show the data ranges of the chemical composition.

Figure 4 shows that the elastic modulus of the TiZrTa alloys varied with the contents of Zr and Ta. According to the diffusion composition profile, the contents of Ta and Zr had an opposite trend. From Figure 4, the elastic modulus first decreased with the increase in Ta and decrease in Zr. With the further increase in Ta and decrease in Zr, the elastic modulus rose. The alloy with a composition of 20.51 at.% Zr and 8.96 at.% Ta had the lowest modulus value of 61.3 GPa. In addition to the lowest point, the alloys with composition 1 (20.85 at.% Zr and 10.55 at.% Ta) and composition 2 (19.72 at.% Zr and 13.61 Ta) also had an elastic modulus lower than 65 GPa (63.7 and 64.8 GPa, respectively). Yan et al. [18] prepared Ti-15Ta-xZr (x = 1.5, 5.5, 10.5, and 15.5 wt.%) alloys with a good biocompatibility by using selective laser melting. Similar to this work, the modulus of the Ti-15Ta-xZr alloy first decreased and then increased with an increase in the Zr content. It is well-known that the elastic modulus of alloys depends on the composition and crystal structure. The elastic modulus of Ti, Zr, and Ta is 102, 68, and 185 GPa, respectively [34]. Based on the rule of the mixture and neglecting the interactions between the elements, the elastic modulus should have decreased with an increase in the content of Zr, but increased with the content of Ta. Correa et al. [35] showed that the elastic modulus of cp-Ti indeed decreased from 105 to 90 GPa by adding 5 wt.% Zr. However, the modulus increased whilst the additional content was over 10 wt.%.
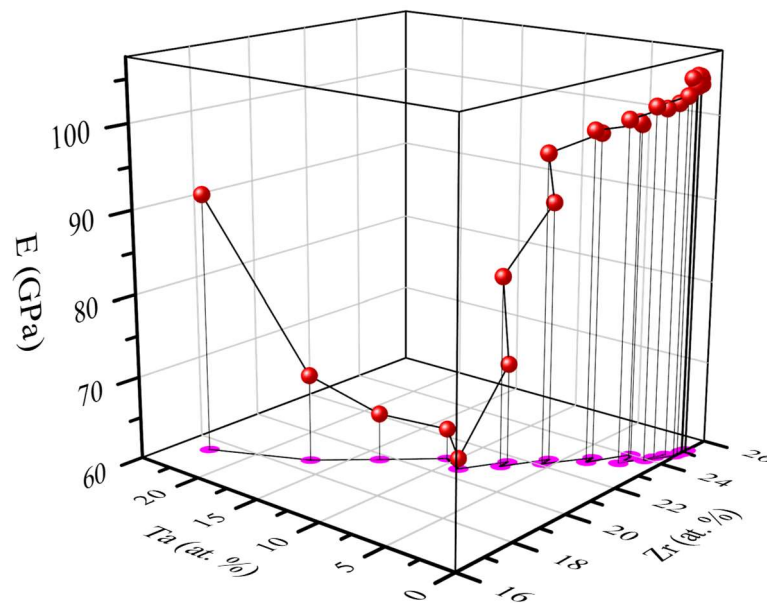
Figure 4. Elastic modulus vs. composition of the TiZrTa alloys. The pink dots are the projection of elastic modulus data on the Zr-Ta alloying composition plane.

Apart from the effect of the composition itself, the addition of Zr and Ta into Ti also changes its crystal structure, which is a more important factor influencing the elastic modulus. Hume-Rothery et al. [36] proved that the crystal structure of alloys depends on the average valence electron per atom, which can also be understood as the free electron-to-atom ratio (e/a). Several researchers have also indicated the e/a ratio value dependence of the crystal structure of Ti alloys. Laheurte et al. [37] supplied the expected structures of Ti alloys after a water quench concerning the electron-to-atom ratio scale, as shown in Figure 5. Moshokoa et al. [38] investigated the effects of the Mo content on the microstructural and mechanical properties of as-cast Ti-Mo alloys and showed that the structure of Ti-Mo binary alloys varies with the e/a ratio value. Xu et al. [39] also indicated that the e/a ratio value influences the phase constitution and, further, the elastic modulus of Ti alloys; they developed a low-cost metastable beta Ti-5Mo-Fe-3Sn Ti alloy with a low elastic modulus and high strength for an orthopedic application. The e/a ratio value of all compositions in this work was calculated. The modulus of the TiZrTa alloys vs. the corresponding e/a ratio values is shown in Figure 6. From 4.0 to 4.50 of the e/a ratio value, the modulus had a small change. This was because the expected structure of the Ti alloys with that e/a range was in the α' phase with an HCP structure, as Figure 5 shows. When the e/a ratio value was over 4.05, the modulus rapidly decreased to 4.09 of the e/a ratio value. In the range from 4.05 to 4.09, the α'' phase started to form and its content became greater with the increase in the e/a ratio value. The composition with the e/a ratio value of 4.09 had the lowest modulus of 61.3 GPa. As the e/a ratio value exceeded 4.09, the modulus increased with the e/a ratio value. Even so, the composition with the e/a ratio value below 4.15 still had a relative low modulus (<70 GPa). A first principles study showed that the Ti alloys with an e/a ratio in the range of 4.06–4.17 were expected to have a low Young's modulus [40]. Hao et al. [41] investigated the elastic deformation behavior of Ti-Nb-Zr-Sn alloys and showed that the alloy with the e/a ratio value of 4.15 had the lowest elastic modulus. The relationship between the elastic modulus of Ti alloys and the e/a ratio value was schematically illustrated, as Figure 7 shows [21]. Speculations about the phase composition in Figure 7 were deduced from the results of the X-ray methods. However, Chen [22] also showed similar phase composition results after measuring the phase composition of a few diffusion couples by using the micro-area measurement method and a focused ion beam. This suggested that the speculations of Figure 7 were also applicable to the micro-area measurement and analysis methods. A comparison of Figure 6 with Figure 7 showed a

similar tendency. However, Figure 6 did not have a second modulus trough with an e/a ratio value near 4.20. That may be because the metastable ω phase could be suppressed in the TiZrTa alloy at the investigated composition range [41].
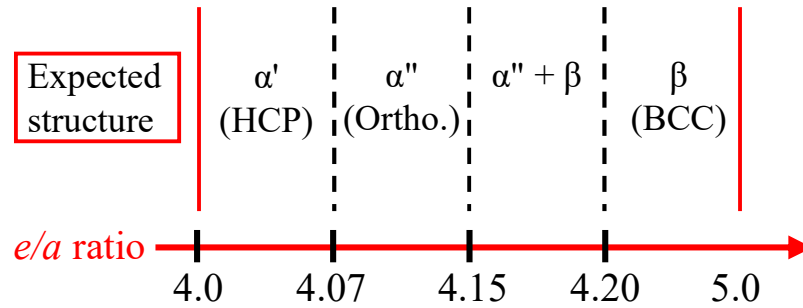

Figure 5. Expected structures of Ti alloys after a water quench with respect to electron-to-atom ratio scale [37].
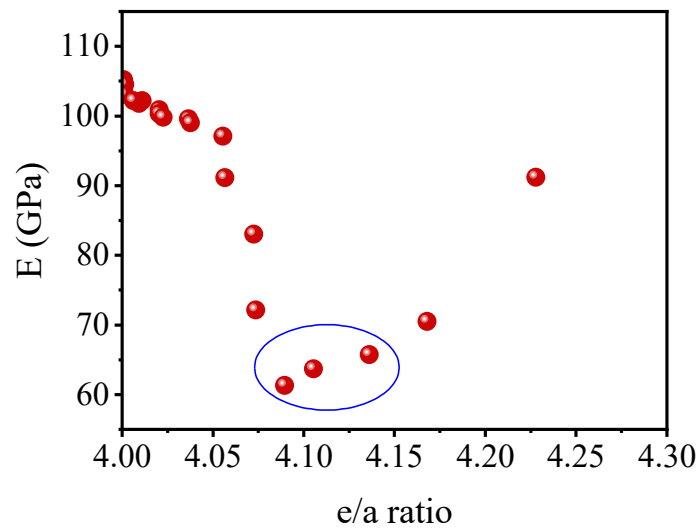

Figure 6. Elastic modulus vs. e/a ratio value of the TiZrTa alloys.
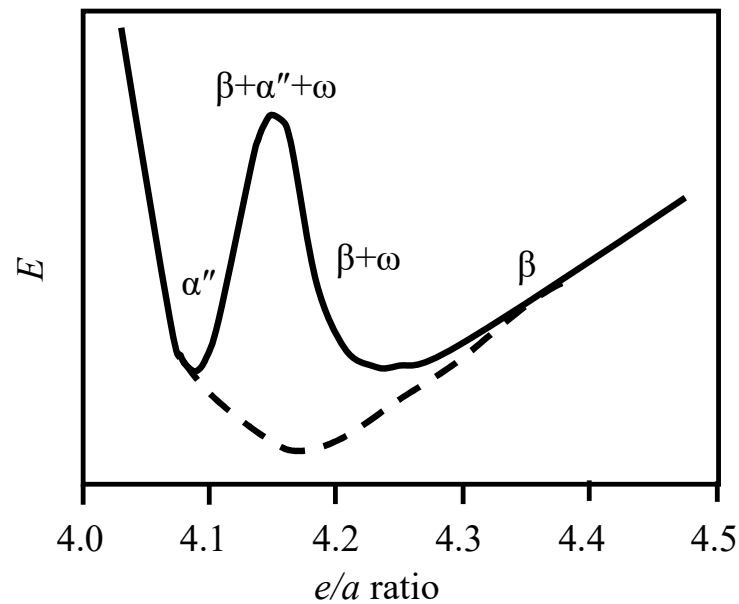

Figure 7. Schematic variation of Young's modulus with e/a ratio in a Ti system [21].

To be a reference and guidance for the development of Ti alloys with a low elastic modulus, our results combined the previously reported data [17–19,42–47] of TiZrTa alloys; the results are shown in Figure 8. The compositions of the TiZrTa alloys in the blue and light blue areas were expected to have a lower modulus. The blue and light blue areas were between the two purple dashed lines. That is, the TiZrTa alloys with a Ta content between 5 and 17.5 at.%, almost regardless of the Zr content (0 to 76 at.% in Figure 8), were likely to have a low modulus. In order to more accurately represent the composition range expected to have a low modulus, those two dashed lines were digitized. The equation of the top dashed purple line—namely, the upper compositional limits of Zr and Ta—could be expressed as Ta = 2.63×10^{-2} Zr + 15. Correspondingly, the lower limit obeyed the equation of Ta = 8.42×10^{-2} Zr + 15. It is well-known that the element of Ta is a typical isomorphous stabilizer of the beta phase for Ti alloys [48]. Thus, a small change in the content of Ta would obviously affect the stability of the beta Ti phase and the formation of the transitional phases of α″ and ω as well. As mentioned above, the stability of the beta phase is a major factor influencing the elastic modulus of Ti alloys. Thus, Ta should be a narrow range for Ti alloys expecting a low elastic modulus. Zr is categorized as the neutral element of Ti alloys [24,48]. Thus, the content of Zr in TiZrTa alloys has a weak effect on the elastic modulus. However, a few publications [49–52] have indicated its beta stabilizing effect when over 10% Zr was added to the Ti alloys. In addition, Liang et al. [25] theoretically showed that the addition of Zr into Ti alloys with one or more beta stabilizers could strengthen the effect of the beta stabilizers. Several experimental results [53–55] have also indicated the same effect of a Zr addition into Ti alloys with beta stabilizers. Thus, as the Zr content increases, the low elastic modulus of TiZrTa alloys needs to decrease the Ta content. That was the reason for the narrower range of the Ta content as the Zr content increased, as the distance between the two purple dashed lines in Figure 8 shows. Marker et al. [56] proposed a variation of Young's modulus with the composition of TiZrTa ternary alloys by a pure theoretical calculation, as Figure 9 shows. The Young's modulus map in Figure 9 shows that the alloys in the Ti corner with Ta < 20 at.% and Zr < 10 at.% or that in the Zr corner with Ta < 25 at.% and Ti < 20 at.% had a modulus below 70 GPa. The range of the Ta content was similar to this work, but the Zr content as different. The reason was that the moduli in Figure 9 were calculated for the pure beta phase. For a few areas, such as near the TiZr binary areas, the beta phase was unstable and could not be retained at room temperature. Thus, the calculated results in those areas was suspicious and further discussion was required. The other key factor of the difference was that there were other phases, such as the α′, α″, and ω phases, in the actual TiZrTa alloys with a low Ta content, not only the beta phase.
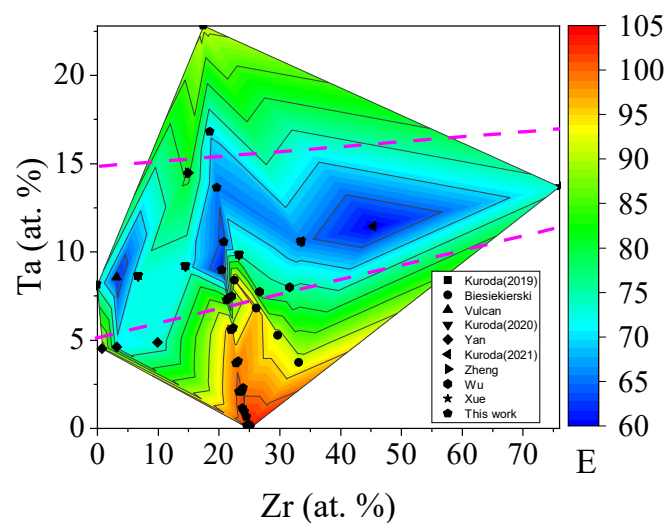

Figure 8. Variation tendency of the elastic modulus of TiZrTa series alloys with contents of Zr and Ta.
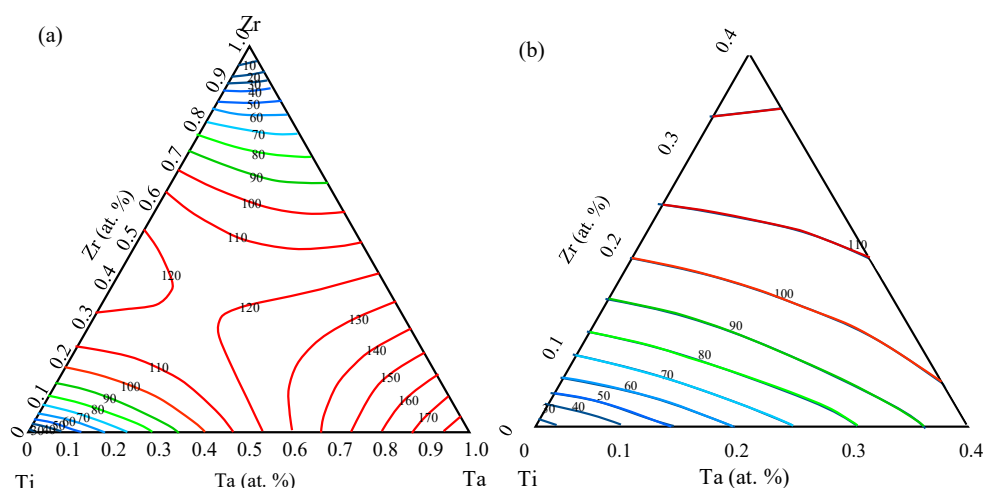
Figure 9. Calculating Young's moduli (**a**) and Ti corner partial image (**b**) of TiZrTa ternary alloys with a pure beta phase [56].

4. Conclusions

The relationship between the composition and elastic modulus of TiZrTa alloys was investigated by using the high-throughput diffusion couple method, nanoindentation, and an electron probe micro-analysis. The main conclusions were as follows.

1. The TiZrTa alloys with a composition of 20.51 at.% Zr and 8.96 at.% Ta had the lowest modulus value of 61.3 GPa. The alloy with the other two compositions, C1 (20.85 at.% Zr and 10.55 at.% Ta) and C2 (19.72 at.% Zr and 13.61 at.% Ta) also had a modulus below 70 GPa.
2. The TiZrTa alloy with the average valence electron per atom value of 4.09 had the lowest elastic modulus. The alloys with an e/a ratio range of 4.09 to 4.15 had a low modulus.
3. The TiZrTa alloys expecting a low elastic modulus should have compositions as follows. The upper content limits of Zr and Ta could be expressed as Ta = 2.63×10^{-2} Zr + 15. Correspondingly, the lower limits obey the equation of Ta = 8.42×10^{-2} Zr + 15.

Author Contributions: Methodology: J.Z. and S.L.; investigation: J.Z., K.L., and M.D.; resources: J.Z. and S.L.; data curation: J.Z. and S.L.; writing—original draft preparation: J.Z.; writing—review and editing: S.L.; project administration: L.Y. All authors have read and agreed to the published version of the manuscript.

Institutional Review Board Statement: Not applicable.

Informed Consent Statement: Not applicable.

Data Availability Statement: The data presented in this study are available on request from the corresponding author.

Conflicts of Interest: The authors declare no conflict of interest.

References

1. Hothan, A.; Lewerenz, K.; Weiss, C.; Hoffmann, N.; Morlock, M.; Huber, G. Vibration transfer in the ball-stem contact interface of artificial hips. *Med. Eng. Phys.* **2013**, *35*, 1513–1517. [CrossRef] [PubMed]
2. McCracken, M. Dental Implant Materials: Commercially Pure Titanium and Titanium Alloys. *J. Prosthodont.* **1999**, *8*, 40–43. [CrossRef] [PubMed]
3. Imam, M.A.; Fraker, A.C. Titanium alloys as implant materials. In *Medical Applications of Titanium and Its Alloys: The Material and Biological Issues*; ASTM International: West Conshohocken, PA, USA, 1996; pp. 3–16.
4. Kuroda, D.; Niinomi, M.; Morinaga, M.; Kato, Y.; Yashiro, T. Design and mechanical properties of new β type titanium alloys for implant materials. *Mater. Sci. Eng. A* **1998**, *243*, 244–249. [CrossRef]
5. Niinomi, M. Mechanical biocompatibilities of titanium alloys for biomedical applications. *J. Mech. Behav. Biomed. Mater.* **2008**, *1*, 30–42. [CrossRef] [PubMed]
6. Niinomi, M.; Nakai, M.; Hieda, J. Development of new metallic alloys for biomedical applications. *Acta Biomater.* **2012**, *8*, 3888–3903. [CrossRef]
7. Niinomi, M.; Nakai, M. Titanium-Based Biomaterials for Preventing Stress Shielding between Implant Devices and Bone. *Int. J. Biomater.* **2011**, *2011*, 836587. [CrossRef]
8. Steinemann, S.G. Corrosion of surgical implants-in vivo and in vitro tests. *Eval. Biomater.* **1980**, *1*, 1–34.
9. Kawara, H. Cytotoxicity of implantable metals and alloy. *Bull. Jpn. Inst. Met.* **1992**, *31*, 1033–1039. [CrossRef]
10. Yu, G.; Li, Z.; Li, S.; Zhang, Q.; Hua, Y.; Liu, H.; Zhao, X.; Dhaidhai, D.T.; Li, W.; Wang, X. The select of internal architecture for porous Ti alloy scaffold: A compromise between mechanical properties and permeability. *Mater. Des.* **2020**, *192*, 108754. [CrossRef]
11. Liang, S.X.; Feng, X.J.; Yin, L.X.; Liu, X.Y.; Ma, M.Z.; Liu, R.P. Development of a new beta Ti alloy with low modulus and favorable plasticity for implant material. *Mater. Sci. Eng. C Mater. Biol. Appl.* **2016**, *61*, 338–343. [CrossRef]
12. Hafeez, N.; Liu, J.; Wang, L.; Wei, D.; Tang, Y.; Lu, W.; Zhang, L.-C. Superelastic response of low-modulus porous beta-type Ti-35Nb-2Ta-3Zr alloy fabricated by laser powder bed fusion. *Addit. Manuf.* **2020**, *34*, 101264. [CrossRef]
13. Li, Y.-H.; Shang, X.-Y. Recent progress in porous TiNb-based alloys for biomedical implant applications. *Mater. Sci. Technol.* **2020**, *36*, 385–392. [CrossRef]
14. Qi, P.; Li, B.; Wang, T.; Zhou, L.; Nie, Z. Microstructure and properties of a novel ternary Ti–6Zr–xFe alloy for biomedical applications. *J. Alloys Compd.* **2021**, *854*, 157119. [CrossRef]
15. Hu, S.; Li, T.; Su, Z.; Liu, D. Research on suitable strength, elastic modulus and abrasion resistance of Ti–Zr–Nb medium entropy alloys (MEAs) for implant adaptation. *Intermetallics* **2022**, *140*, 107401. [CrossRef]
16. Shi, Y.D.; Wang, L.N.; Liang, S.X.; Zhou, Q.; Zheng, B. A high Zr-containing Ti-based alloy with ultralow Young's modulus and ultrahigh strength and elastic admissible strain. *Mater. Sci. Eng. A* **2016**, *674*, 696–700. [CrossRef]
17. Kuroda, P.A.B.; de Freitas Quadros, F.; Sousa, K.d.S.J.; Donato, T.A.G.; de Araújo, R.O.; Grandini, C.R. Preparation, structural, microstructural, mechanical and cytotoxic characterization of as-cast Ti-25Ta-Zr alloys. *J. Mater. Sci. Mater. M* **2020**, *31*, 19. [CrossRef]
18. Yan, L.; Yuan, Y.; Ouyang, L.; Li, H.; Mirzasadeghi, A.; Li, L. Improved mechanical properties of the new Ti-15Ta-xZr alloys fabricated by selective laser melting for biomedical application. *J. Alloys Compd.* **2016**, *688*, 156–162. [CrossRef]
19. Zheng, X.H.; Ning, R.; Tan, C.L.; Huang, S.; Zhang, Z.G.; Cai, W. The effects of indium addition on mechanical properties and shape memory behavior of Ti-Ta-Zr high temperature alloys. *Mater. Chem. Phys.* **2020**, *249*, 123189. [CrossRef]
20. Popov, A.A.; Illarionov, A.G.; Grib, S.V.; Elkina, O.A.; Ivasishin, O.M.; Markovskii, P.E.; Skiba, I.A. Effect of heat treatment and plastic deformation on the structure and elastic modulus of a biocompatible alloy based on zirconium and titanium. *Phys. Met. Metallogr.* **2012**, *113*, 382–390. [CrossRef]
21. Liang, S. Review of the Design of Titanium Alloys with Low Elastic Modulus as Implant Materials. *Adv. Eng. Mater.* **2020**, *22*, 2000555. [CrossRef]
22. Chen, Z. A Comprehensive Study of Diffusion and Modulus of Binary Systems within the Ti-Mo-Nb-Ta-Zr System. Ph.D. Thesis, The Ohio State University, Columbus, OH, USA, 2019.
23. Ling, J.; Huang, D.; Bai, K.; Li, W.; Yu, Z.; Chen, W. High-throughput development and applications of the compositional mechanical property map of the β titanium alloys. *J. Mater. Sci. Technol.* **2021**, *71*, 201–210. [CrossRef]
24. Wang, B.; Ruan, W.; Liu, J.; Zhang, T.; Yang, H.; Ruan, J. Microstructure, mechanical properties, and preliminary biocompatibility evaluation of binary Ti-Zr alloys for dental application. *J. Biomater. Appl.* **2019**, *33*, 766–775. [CrossRef] [PubMed]
25. Liang, S.; Zhou, Y.; Yin, L. Strengthening/Weakening Action of Zr on Stabilizers of Ti Alloys and Its Effect on Phase Transition. *J. Mater. Eng. Perform.* **2021**, *30*, 876–884. [CrossRef]
26. Aniskin, M.V.; Ignatova, O.N.; Kaganova, I.I.; Kalmanov, A.V.; Koshatova, E.V.; Lebedev, A.I.; Losev, V.V.; Podurets, A.M.; Polyakov, L.V.; Tkachenko, M.I.; et al. Mechanical properties of tantalum with different types of microstructure under high-rate deformation. *Phys. Mesomech.* **2011**, *14*, 79–84. [CrossRef]
27. Oliver, W.; Pharr, G. An Improved Technique for Determining Hardness and Elastic Modulus Using Load and Displacement Sensing Indentation Experiments. *J. Mater. Res.* **1992**, *7*, 1564–1583. [CrossRef]
28. Oliver, W.; Pharr, G.M. Measurement of hardness and elastic modulus by instrumented indentation. *J. Mater. Res.* **2004**, *19*, 3–20. [CrossRef]

29. Zareidoost, A.; Yousefpour, M. A study on the mechanical properties and corrosion behavior of the new as-cast TZNT alloys for biomedical applications. *Mater. Sci. Eng. C* **2020**, *110*, 110725. [CrossRef] [PubMed]

30. Zhao, Y.; Singaravelu, A.S.S.; Ma, X.; Liu, X.; Chawla, N. Mechanical properties of Al3BC by nanoindentation and micropillar compression. *Mater. Lett.* **2020**, *264*, 127361. [CrossRef]

31. Kim, S.-P.; Kaseem, M.; Choe, H.-C. Plasma electrolytic oxidation of Ti-25Nb-xTa alloys in solution containing Ca and P ions. *Surf. Coat. Technol.* **2020**, *395*, 125916. [CrossRef]

32. Liu, Y.; Zhang, L.; Du, Y.; Wang, J.; Liang, D. Study of atomic mobilities and diffusion characteristics in bcc Ti–Ta and Ta–W alloys. *Calphad* **2010**, *34*, 310–316. [CrossRef]

33. Ansel, D.; Thibon, I.; Boliveau, M.; Debuigne, J. Interdiffusion in the body cubic centeredβ-phase of Ta–Ti alloys. *Acta Mater.* **1998**, *46*, 423–430. [CrossRef]

34. Martienssen, W. *Springer Handbook of Condensed Matter and Materials Data*, 1st ed.; Martienssen, W., Warlimont, H., Eds.; Springer: Berlin/Heidelberg, Germany, 2005.

35. Correa, D.R.N.; Vicente, F.B.; Donato, T.A.G.; Arana-Chavez, V.E.; Buzalaf, M.A.R.; Grandini, C.R. The effect of the solute on the structure, selected mechanical properties, and biocompatibility of Ti–Zr system alloys for dental applications. *Mater. Sci. Eng. C.* **2014**, *34*, 354–359. [CrossRef] [PubMed]

36. Hume-Rothery, W.; Mabbott, G.W.; Channel Evans, K.M.; Carpenter, H.C.H. The freezing points, melting points, and solid solubility limits of the alloys of sliver and copper with the elements of the b sub-groups. *Philos. Trans. R. Soc. Lond. Ser. A Contain. Pap. A Math. Phys. Character* **1934**, *233*, 1–97.

37. Laheurte, P.; Prima, F.; Eberhardt, A.; Gloriant, T.; Wary, M.; Patoor, E. Mechanical properties of low modulus β titanium alloys designed from the electronic approach. *J. Mech. Behav. Biomed. Mater.* **2010**, *3*, 565–573. [CrossRef] [PubMed]

38. Moshokoa, N.; Raganya, L.; Obadele, B.; Olubambi, P.; Machaka, R. Effects of Mo content on the microstructural and mechanical properties of as-cast Ti-Mo alloys. *IOP Conf. Ser. Mater. Sci. Eng.* **2019**, *655*, 012015. [CrossRef]

39. Xu, Y.; Gao, J.; Huang, Y.; Rainforth, W.M. A low-cost metastable beta Ti alloy with high elastic admissible strain and enhanced ductility for orthopaedic application. *J. Alloys Compd.* **2020**, *835*, 155391. [CrossRef]

40. You, L.; Song, X. First principles study of low Young's modulus Ti–Nb–Zr alloy system. *Mater. Lett.* **2012**, *80*, 165–167. [CrossRef]

41. Hao, Y.L.; Li, S.J.; Sun, S.Y.; Zheng, C.Y.; Yang, R. Elastic deformation behaviour of Ti-24Nb-4Zr-7.9Sn for biomedical applications. *Acta Biomater.* **2007**, *3*, 277–286. [CrossRef]

42. Biesiekierski, A.; Ping, D.; Li, Y.; Lin, J.; Munir, K.S.; Yamabe-Mitarai, Y.; Wen, C. Extraordinary high strength Ti-Zr-Ta alloys through nanoscaled, dual-cubic spinodal reinforcement. *Acta Biomater.* **2017**, *53*, 549–558. [CrossRef] [PubMed]

43. Vulcan, A.D.; Răducanu, D.; Cojocaru, V.D.; Cincă, I. The evolution of mechanical characteristics for a thermomechanical processed Ti-Ta-Zr alloy. *UPB Sci. Bull. Ser. B Chem. Mater. Sci.* **2011**, *73*, 229–236.

44. Kuroda, P.A.B.; Quadros, F.d.F.; Afonso, C.R.M.; Grandini, C.R. The Effect of Solution Heat Treatment Temperature on Phase Transformations, Microstructure and Properties of Ti-25Ta-xZr Alloys Used as a Biomaterial. *J. Mater. Eng. Perform.* **2020**, *29*, 2410–2417. [CrossRef]

45. Kuroda, P.A.B.; Pedroso, B.L.T.; Pontes, F.M.L.; Grandini, C.R. Effect of Titanium Addition on the Structure, Microstructure, and Selected Mechanical Properties of As-Cast Zr-25Ta-xTi Alloys. *Metals* **2021**, *11*, 1507. [CrossRef]

46. Wu, R.; Yi, Q.; Lei, S.; Dai, Y.; Lin, J. Design of Ti-Zr-Ta Alloys with Low Elastic Modulus Reinforced by Spinodal Decomposition. *Coatings* **2022**, *12*, 756. [CrossRef]

47. Xue, G.-l.; Yang, H.-l.; Xing, H.-x.; Ye, C.-r.; Liu, J.; Miao, J.-l.; Ruan, J.-m. Effect of Ti on microstructure, mechanical properties and corrosion resistance of Zr-Ta-Ti alloys processed by spark plasma sintering. *J. Cent. South Univ.* **2020**, *27*, 2185–2197. [CrossRef]

48. Biesiekierski, A.; Wang, J.; Abdel-Hady Gepreel, M.; Wen, C. A new look at biomedical Ti-based shape memory alloys. *Acta Biomater.* **2012**, *8*, 1661–1669. [CrossRef] [PubMed]

49. Liang, S.X.; Ma, M.Z.; Jing, R.; Zhang, X.Y.; Liu, R.P. Microstructure and mechanical properties of hot-rolled ZrTiAlV alloys. *Mater. Sci. Eng. A* **2012**, *532*, 1–5. [CrossRef]

50. Jing, R.; Liang, S.X.; Liu, C.Y.; Ma, M.Z.; Zhang, X.Y.; Liu, R.P. Structure and mechanical properties of Ti–6Al–4V alloy after zirconium addition. *Mater. Sci. Eng. A* **2012**, *552*, 295–300. [CrossRef]

51. Jiang, J.; Zhou, C.; Zhao, Y.; He, F.; Wang, X. Development and properties of dental Ti–Zr binary alloys. *J. Mech. Behav. Biomed. Mater.* **2020**, *112*, 104048. [CrossRef]

52. Yu, Q.; Wang, C.; Wang, D.; Min, X. Microstructure and properties of Ti–Zr congruent alloy fabricated by laser additive manufacturing. *J. Alloys Compd.* **2020**, *834*, 155087. [CrossRef]

53. Gouda, M.K.; Salman, S.A.; Ebied, S.; Ashmawy, A.M.; Gepreel, M.A.H.; Chiba, A. Biocompatibility and corrosion resistance of low-cost Ti–14Mn–Zr alloys. *J. Mater. Res.* **2021**, *36*, 4883–4893. [CrossRef]

54. Martins, D.Q.; Osório, W.R.; Souza, M.E.P.; Caram, R.; Garcia, A. Effects of Zr content on microstructure and corrosion resistance of Ti–30Nb–Zr casting alloys for biomedical applications. *Electrochim. Acta* **2008**, *53*, 2809–2817. [CrossRef]

55. Abdel-Hady, M.; Fuwa, H.; Hinoshita, K.; Kimura, H.; Shinzato, Y.; Morinaga, M. Phase stability change with Zr content in β-type Ti–Nb alloys. *Scripta Mater.* **2007**, *57*, 1000–1003. [CrossRef]

56. Marker, C.; Shang, S.-L.; Zhao, J.-C.; Liu, Z.-K. Elastic knowledge base of bcc Ti alloys from first-principles calculations and CALPHAD-based modeling. *Comput. Mater. Sci.* **2017**, *140*, 121–139. [CrossRef]